Available online at www.sciencedirect.com

SCIENCE DIRECT®

Lithos 77 (2004) 375–393

LITHOS

www.elsevier.com/locate/lithos

Mildly incompatible elements in peridotites and the origins of mantle lithosphere☆

Dante Canil*

School of Earth and Ocean Sciences, University of Victoria, Petch building, Room 280, 3800 Finnerty Rd., Victoria, BC, Canada V8W 3P6

Received 27 June 2003; accepted 4 February 2004
Available online 15 June 2004

Abstract

The abundances of the mildly incompatible elements Al, Cr, V, Sc and Yb in more than 1700 mantle peridotite bulk rock analyses are interpreted in the light of a fractional melting model based on experimentally measured partition coefficients (D) and melting reaction stoichiometries. All peridotites examined, irrespective of sample type (abyssal peridotites, orogenic massifs, ophiolites, on/off craton xenoliths), tectonic environment (divergent/convergent/passive margin, intraplate) or the pressure (P) they last equilibrated at in the mantle (plagioclase-, spinel- , or garnet facies), originated as residues at less than 3 GPa, mainly within the spinel-facies. Mantle rocks currently in the garnet facies likely were originally spinel-facies lithosphere underthrust or subducted to greater depths in convergent margins. This view is inescapable even within the widest range of D values employed in the calculations, and is furthermore strengthened when metasomatic effects on the abundances of the mildly incompatible elements in residues are considered. A pressure of origin of below $\sim$ 3 GPa for most mantle lithosphere creates difficulties for any model ascribing a significant volume of deep, cratonic mantle roots to plume sub-cretion or any other vertical tectonic mechanism.

Keywords: Mantle; Lithosphere; Peridotite; Melting; Trace element; Geochemistry; Modeling

1. Introduction

The composition of mantle lithosphere dictates its thermal and mechanical properties, stability and lifetime during the geodynamic evolution of our planet (Jordan, 1975; Poudjom Djomani et al., 2001). It would be useful to know or predict if fundamentally different compositions of mantle lithosphere are produced in different settings, and if so, why, and how they control the greater dynamics of continental and oceanic plates of varying age and tectonothermal history.

A wealth of information about the composition of the mantle lithosphere can be obtained from the study of hundreds of volcanic-hosted xenoliths (Griffin et al., 1999a; Jagoutz et al., 1979; Maaloe and Aoki, 1977; McDonough and Sun, 1995; Pearson et al., 2003). Although xenoliths can be placed into a spatial context in the mantle, they are accidental samples when entrained by their host magma, and age information and their original tectonic environment of formation is often obscure. In contrast, samples of the mantle in outcrop as orogenic massifs, ophiolites and dredged from the modern ocean basins provide a large in situ example of lithosphere in contrasting tectonic settings,

☆ Supplementary data associated with this article can be found, in the online version, at doi: 10.1016/j.lithos.2004.04.014.

* Tel.: +1-250-472-4180; fax: +1-250-721-6200.
E-mail address: dcanil@uvic.ca (D. Canil).

0024-4937/$ - see front matter © 2004 Elsevier B.V. All rights reserved.
doi:10.1016/j.lithos.2004.04.014

Table 2
Data sources to world peridotite compilation

Peridotite type	Data source
Samples in 'Outcrop'	
Abyssal	Aumento and Loubat (1971)
	Brandon et al. (2000)
	Casey (1997)
	Coogan et al. (in press)
	Gillis et al. (1993)
	Miyashiro et al. (1969)
	Niu and Hekinian (1997)
	Prinz et al. (1976)
	Snow and Dick (1995)
	Stephens (1997)
Ophiolite	Berry (1981)
	Coogan et al. (in press)
	Gruau et al. (1991)
	Gruau et al. (1998)
	Jaques and Chappell (1980)
	Loney et al. (1971)
	Rampone et al. (1993)
	Rampone et al. (1996)
	Zhou et al. (1996)
Forearc	Parkinson and Pearce (1998)
	Pearce et al. (2000)
Orogenic Massif	Becker (1996)
	Bodinier (1988)
	Bodinier et al. (1988)
	Burnham et al. (1998)
	Canil et al. (2003)
	Chauvel and Jahn (1984)
	Ernst (1978)
	Fabries et al. (1991)
	Frey et al. (1985)
	Gueddari et al. (1996)
	Hartmann and Wedepohl (1993)
	McPherson et al. (1996)
	Scambelluri et al. (2001)
	Shervais and Mukasa (1991)
	Takazawa et al. (2000)
Passive margin	Bonatti et al. (1986)
	Seifert and Brunotte (1996)
	Zhang et al. (2000)
Xenoliths	
Cratonic xenolith	Bernstein et al. (1998)
	Boyd and Mertzman (1987)
	Boyd et al. (1993)
	Boyd et al. (1997)
	Boyd (1999)
	Carlson et al. (1999)
	Jaques et al. (1990)
	Kopylova and Russell (2000)
	Lee and Rudnick (1999)
	Peltonen et al. (1999)
	Rudnick et al. (1993)
	Schmidberger and Francis (2001)
	Winterburn et al. (1990)
Xenoliths	
Ocean Island	Ehrenberg (1982)
	Gregoire et al. (2000)
	Hauri et al. (1993)
	Siena et al. (1991)
Cont. Rift	Bedini et al. (1997)
	Ionov et al. (1993)
	Press et al. (1986)
Cont. Intraplate	Aoki (1981)
	Dautria and Girod (1986)
	Dautria et al. (1992)
	Dupuy et al. (1987)
	Embey-Isztin et al. (1989)
	Francis (1987)
	Frey and Green (1974)
	Griffin et al. (1987)
	Hunter and Upton (1987)
	Jagoutz et al. (1979)
	Laurora et al. (2001)
	Lee et al. (2003)
	Lenoir et al. (2000)
	Lenoir et al. (2001)
	Menzies and Hawkesworth (1987)
	Morten (1987)
	Peslier et al. (2002)
	Qi et al. (1995)
	Shi et al. (1998)
	Smith and Levy (1976)
	Smith et al. (1999)
	Song and Frey (1989)
	Stolz and Davies (1991)
	Vaselli et al. (1995)
	Xue et al. (1990)
	Yaxley et al. (1998)
	Zangana et al. (1999)
Cont. Arc	Liang and Elthon (1990)
	Luhr and Aranda-Gomez (1997)
Oceanic Arc	Franz et al. (2002)
	Maury et al. (1992)
	McInnes et al. (2001)

usually of known age, but are less frequently sampled and may also undergo modification when exhumed or exposed in environments with complex geological histories.

This contribution examines a large data compilation of the bulk composition of mantle peridotites in outcrop and as xenoliths from a range of tectonic settings. The database is used in concert with experimentally measured partition coefficients (D) and mantle melting

reactions, to distinguish the pressure (P) and oxygen fugacity (fO_2) of melting and potentially the tectonic environment for the formation of lithosphere later sampled accidentally as xenoliths in alkaline magmas.

2. The mantle peridotite data set

More than 1700 peridotite bulk rock analyses were compiled from over 80 data sources in the literature. Similar though less extensive compilations have been published previously (Hart and Zindler, 1986; Maaloe and Aoki, 1977; McDonough and Sun, 1995; Palme and Nickel, 1985), but in this case a full table of analyses (Table 1) is available as a supplementary online electronic data set accessible via the Elsevier/Lithos website. The main focus here is on the abundances of Al, Cr, Sc, V and Yb because they are mildly incompatible elements less affected by metasomatism, as will be shown below.

All data sources are post-1969. In all cases, element concentrations were determined by X-ray fluorescence (XRF), neutron activation or inductively coupled plasma mass spectrometry (ICPMS). Unfortunately, Sc, V and Yb are not always analysed in the same or all samples in a suite. Interlaboratory consistency or accuracy for these elements is not always demonstrable and no robust assessment of this issue can be presented at this time. Problems arise from this because some peridotites have V or Sc contents near the typical detection limits for these elements using XRF (~ 10 ppm). A recent assessment by Lee et al. (2003) for V showed that this element is likely known to within 10% relative.

The peridotite samples were divided according to the tectonic environment in which they were sampled either in outcrop or as accidental xenoliths in volcanic rocks (Table 2). High-temperature peridotites with 'sheared' or porphyroclastic textures derived from kimberlites are often strongly overprinted by trace element budgets related to melt-metasomatism and are excluded from this study. Some tectonic environments are not well represented (e.g., forearc exposures, arc xenoliths), mainly due to a lack of studies in the literature. Nonetheless, the division of tectonic environments shows a good correlation with the average

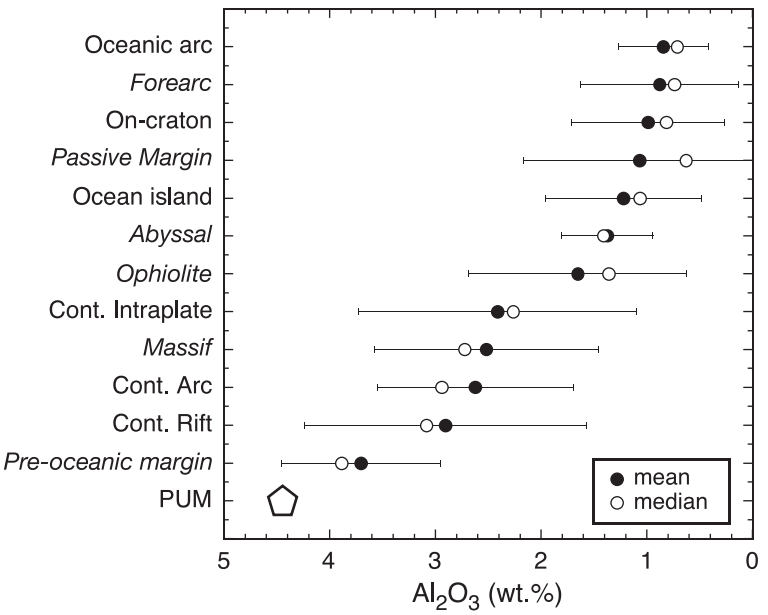

Fig. 1. The median and mean level of depletion (Al_2O_3 content) of mantle peridotites in the data compilation from this study (n>1700), classified according to the tectonic environment in which they were sampled. Samples from outcrop are listed in italics, all others are xenolith data. Error bars are one standard deviation of the mean. The composition of primitive upper mantle (PUM) used in this and subsequent figures is from McDonough and Sun (1995).

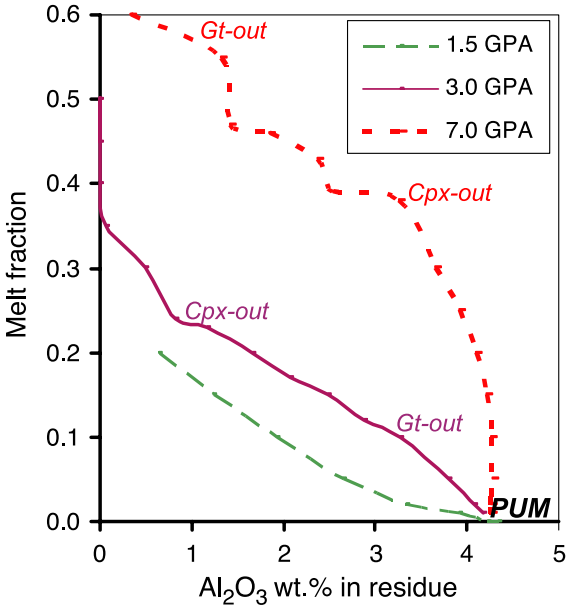

Fig. 2. Al_2O_3 contents in peridotite residues as a function of melt fraction (F) at pressures of 1.5, 3.0 and 7.0 GPa. Trends are calculated using a fractional melting model in which Al is treated as a mildly incompatible element, with primitive upper mantle (PUM) as the source material. Bulk $D_{Al_2O_3}$ residue/liq is parameterized as a function of (F) using chemical data from peridotite melting experiments and weighted according to experimentally determined stoichiometry of melting reactions (see Canil, 2002 for details). The inflections in the melting trends at each pressure correspond to consumption of a phase and corresponding change in the stoichiometry of the melting reaction. Note that although garnet is stable on the solidus at 3.0 GPa, it is consumed at ~ 10% melting, corresponding to ~ 3.5 wt.% Al_2O_3 in the residue.

level of depletion as indexed by the bulk rock Al_2O_3 content (Fig. 1). Al_2O_3 is used as a depletion index because it is immobile during metamorphism and allows for comparison of samples from all states of preservation. Moreover, the behaviour of Al_2O_3 during partial melting is sensitive to P (Herzberg, 1995; Walter, 1998) and simple to model empirically with experimental data on peridotite melting (Fig. 2).

3. Empirical partial melting model

Experimentally measured element partition coefficients (D) in mafic and ultramafic systems (Table 3, Fig. 3) are used in a fractional melting model (Johnson et al., 1990) that weights the D's according to the stoichiometry of the melting reactions along the peridotite solidus, also determined by experiment. This empirical melting model is described in detail in Canil (2002) and used to derive the composition of residues as functions of P, degree of melting and, in the case of V, oxygen fugacity (fO_2). Because experimentally measured D values vary considerably (by factors of 2 to 5), the melting models used to derive residue trends in this study were calculated as end-member cases (i.e., highest and lowest D) for comparison with chemical data for mantle residues. The elements Yb, Cr, Sc and V all partition differently amongst key mantle minerals (garnet, spinel, clinopyroxene, orthopyroxene, olivine) involved during the partial melting of peridotite (Table 3). Of these elements, V is redox sensitive, and the order of partition differs, with the general relation: $D_{gt/liq} > D_{cpx/liq} \gg D_{sp/liq}$ for Sc and Yb; $D_{sp/liq} > D_{cpx/liq} \gg D_{gt/liq}$ for V; $D_{sp/liq} \gg D_{cpx/liq} > D_{gt/liq}$ for Cr. Thus, correlations amongst Yb, Cr, Sc, V and Al are predicted to be illustrative of the effects of P, fO_2 and extent of melting to form a peridotite residue.

4. Effects of metasomatism

Numerous isotopic and trace element studies have revealed that all examples of mantle lithosphere have suffered some degree of chemical modification (metasomatism) that post-dates the original melting process. An assessment of the impact of metasomatic processes on the bulk rock chemistry of samples considered in this study is required to evaluate the degree to which they retain their chemical signature as residues.

Elements that are highly incompatible are most compromised by metasomatism, either over long periods in the lithosphere or immediately prior to or during entrainment in their host magma. The residence of many highly incompatible elements (bulk $D < 0.01$) is dominated by minor phases and grain boundary phenomena, some of which are introduced by entrainment in the host magma (Pearson et al., 2003). For this reason, this study does not concern itself with highly incompatible elements. The main focus here is on Al, Cr, Sc, V and Yb, because these elements generally have a bulk D (residue/liq) between 1 and 0.1 and thus their abundances should be less affected by chemical modifications impregnated

Table 3
Data sources for partition coefficients

Mineral	Bulk comp.	Element	*D* value	Data source
Garnet	komatiite	Sc	1.1	Yurimoto and Ohtani, 1992
	basalt	Sc	2.62	Hauri et al., 1994
	komatiite	Yb	0.9	Yurimoto and Ohtani, 1992
	basalt	Yb	6.6	Johnson, 1998
	peridotite	V	**	Canil, 2002
Clinopyroxene	picrite	Sc	0.51	Ulmer, 1989
	basalt	Sc	1.31	Hart and Dunn, 1993
	basalt	Yb	0.22	Gaetani and Grove, 1995
	basalt	Yb	0.623	Hauri et al., 1994
	Ab-An-Di	V	**	Canil and Fedortchouk, 2000
	basalt	V	**	Canil and Fedortchouk, 2000
Olivine	basalt	Sc	0.12	Beattie, 1994
	chondrule	Sc	0.47	Kennedy et al., 1992
	basalt	Yb	0.0157	Beattie, 1994
	chondrule	Yb	0.017	Kennedy et al., 1992
	komatiite	V	**	Canil and Fedortchouk, 2001
Low Ca Pyroxene	picrite	Sc	0.33	Ulmer, 1989
	chondrule	Sc	0.48	Kennedy et al., 1992
	chondrule	Yb	0.032	Kennedy et al., 1992
	basalt	Yb	0.08	Schwandt and McKay, 1998
	chondrule	V	**	Canil, 1999
Spinel	Fo-An-Di	Sc	0.36	Horn et al., 1994
	synthetic	Sc	0.0478	Nagasawa et al., 1980
	basalt	Yb	0.01	McKenzie and O'Nions, 1991
	synthetic	Yb	0.0076	Nagasawa et al., 1980
	komatiite	V	**	Canil, 2002

***D* values for V vary with fO_2 according to relationships given in the data source. See Fig. 2 for range of *D*.

upon mantle peridotites during their residence in the lithosphere, as is demonstrated with detailed studies of the metasomatic process.

A well-constrained study of metasomatism at the outcrop scale by McPherson et al. (1996) examined trace element abundances in peridotite surrounding amphibole-bearing veins in the Lherz orogenic massif. The veins were interpreted to be channels for melt that percolated outward into the host peridotite creating a metasomatic front. Fig. 4 shows no real change can be discerned for whole rock abundances of Sc, V, Al and Cr (not shown) with distance from the veins into the host peridotite. Only the most incompatible Yb has been disturbed, but only for small mantle volumes near the veins. This example shows that metasomatism may only serve to inflate the concentrations of all incom-

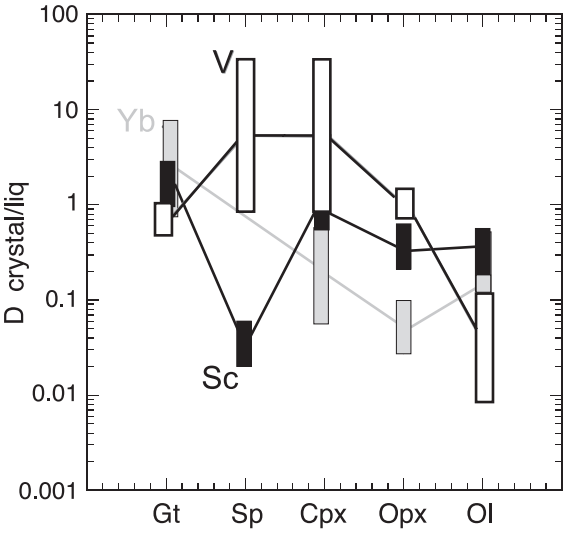

Fig. 3. End-member (highest and lowest) partition coefficients (*D*) measured experimentally for mantle minerals in mafic and ultramafic systems (Table 3). Note the order of partition for these mildly incompatible elements differs for each phase. The spread in V is due its change with fO_2 (Table 3).

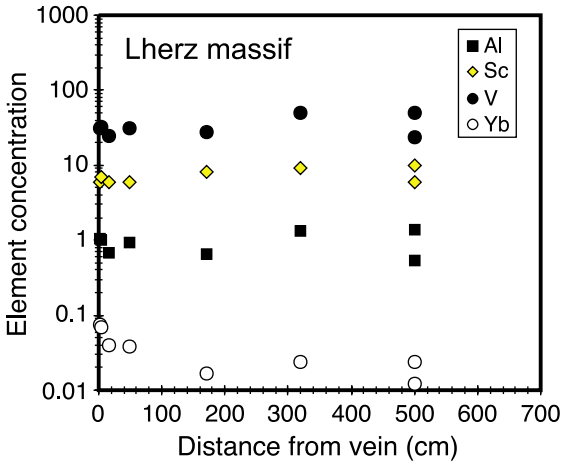

Fig. 4. Chemical data for peridotites sampled in outcrop at intervals away from metasomatic veins in the Lherz orogenic peridotite massif, France (McPherson et al., 1996). Note little change in Al, V and Ti (used as a proxy for Sc) away from the veins, and inflation of Yb relative to the former three elements, but only within a decimeter scale near the veins. Data for Cr are not shown to reduce the scale but show an identical trend to Al.

patible elements relative to the original residue, and will preferentially increase the abundances of Yb relative to Al, V, Sc or Cr.

Grain-scale heterogeneity in trace and major elements suggests that many mantle samples contain too much garnet and pyroxene for their degree of depletion, and have experienced addition of these components to an original residue, in some cases shortly before or during entrainment in their host magma (Griffin et al., 1999a,b; Pearson et al., 2002; Simon et al., 2003). The degree to which clinopyroxene and garnet components in mantle rocks are not primary and have been introduced to a residue during its residence in the lithosphere needs to be evaluated because the budgets of Al, Yb, Sc, Cr and V in bulk rock peridotites are dominated by these phases (e.g., Glaser et al., 1999; Schmidberger and Francis, 2001). The modes of clinopyroxene and garnet in highly depleted rocks are only adequately sampled in large specimens (Boyd and Mertzman, 1987), so only high-quality data from large samples is useful in this analysis. Fig. 5 shows the observed modes of these rocks compared with those expected from a partial melting model. Such a comparison is only semi-quantitative because modes of clinopyroxene and garnet in a melting model are dependent on starting compositions, and are lower than those recorded in natural samples equilibrated at temperatures below the solidus.

Most residues with greater than 2 wt.% Al_2O_3 do not contain inordinate amounts of clinopyroxene, whereas those with less than ~1.5 wt.% Al_2O_3 contain an excess of several percent (Fig. 5). A similar trend is observed by Pearson et al. (2002) using a different melting model and Mg# as a depletion index. The origin of the excess clinopyroxene in such rocks has been debated. Such residues may have cooled to form clinopyroxene from higher temperature Ca- and Al-rich pyroxene above the solidus, as originally proposed on textural grounds (Cox et al., 1987) and demonstrated by experiment (Canil, 1991). More quantitative mass balance and consideration of trace element abundances and heterogeneity show that exsolution does not account for sufficient clinopyroxene in these rocks, and that much of this clinopyroxene is instead "added" to a residue (Boyd and Mertzman, 1987; Canil, 1992; Shimizu et al., 1997; Simon et al., 2003). This would explain the scatter of clinopyroxene abundance in residues showing a range of depletion (e.g., Al_2O_3 content—Fig. 5). The effect of this added clinopyroxene on trace element abundances is evaluated further below.

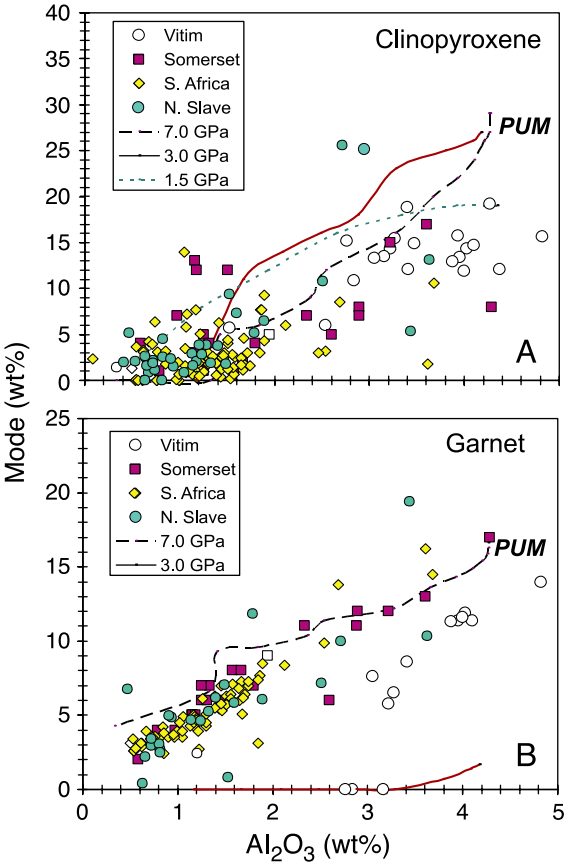

Fig. 5. Modal garnet and clinopyroxene in large (>500 g) samples of cratonic garnet peridotites from Vitim, the northern Slave, Kaapvaal and Somerset Island, Canada plotted against Al_2O_3 (see Table 2 for references). The latter element is used as a depletion index. Partial melting trends assuming a primitive upper mantle starting material (PUM) are based on the same model detailed in Canil (2002) and summarized in Fig. 2. Note the regular change in garnet, but relative scatter in clinopyroxene, with depletion. Peridotites with less than ~1.5 wt.% Al_2O_3 appear to contain clinopyroxene and or garnet in excess of that predicted by their degree of depletion by partial melting.

The presence of garnet overgrowths in several studies shows that some component of this phase has also been introduced in the mantle lithosphere. No study has yet provided a quantitative estimate of the total mass of garnet added to a mantle rock by metasomatism, relative to the amount originally present. A survey of the size of metasomatic garnet overgrowths described in the literature (Smith et al.,

1991; Smith and Boyd, 1992; Griffin et al., 1999a,b; Simon et al., 2003) suggest that 40% to 70% of the volume of garnet was added in one or more metasomatic processes. This figure is determined by approximating the garnets as spheres and using the grain radii reported in these studies to calculate relative volumes of the original core and the overgrown rims. The volumes of the overgrowths are maxima because the garnets were assumed to have been sectioned in their geometric center, which is not likely the case.

Some authors report garnet in excess of that expected for a given degree of depletion (Pearson et al., 2002), but comparing observed modes to partial melting trends shows that garnet shows a very regular trend with depletion (Fig. 5B), rather than a scatter as observed for clinopyroxene. As in the case of clinopyroxene, the spatial association of garnet and orthopyroxene in some mantle specimens has led to the proposal for an exsolution origin from high Ca–Al orthopyroxene. Experiments on a typical cratonic peridotite residue with only 1.5 wt.% Al_2O_3 show exsolution of 3% to 7% garnet during cooling (Canil, 1991), similar to that actually observed in modes of these rocks (Fig. 5). The mass balance for exsolution of garnet also fits much better than for clinopyroxene (Canil, 1992; Simon et al., 2003).

Estimates of the effect of garnet and clinopyroxene component, if added by metasomatism, on the abundances of mildly incompatible trace elements can be made in some well-characterized, large garnet peridotites from the Nikos kimberlite, Somerset Island, Canada, for which modes, and trace element abundances in garnet, clinopyroxene and bulk rocks are known (Schmidberger and Francis, 2001). In this example, the authors did not analyze for Sc–Ti is substituted as an element with broadly similar behav-

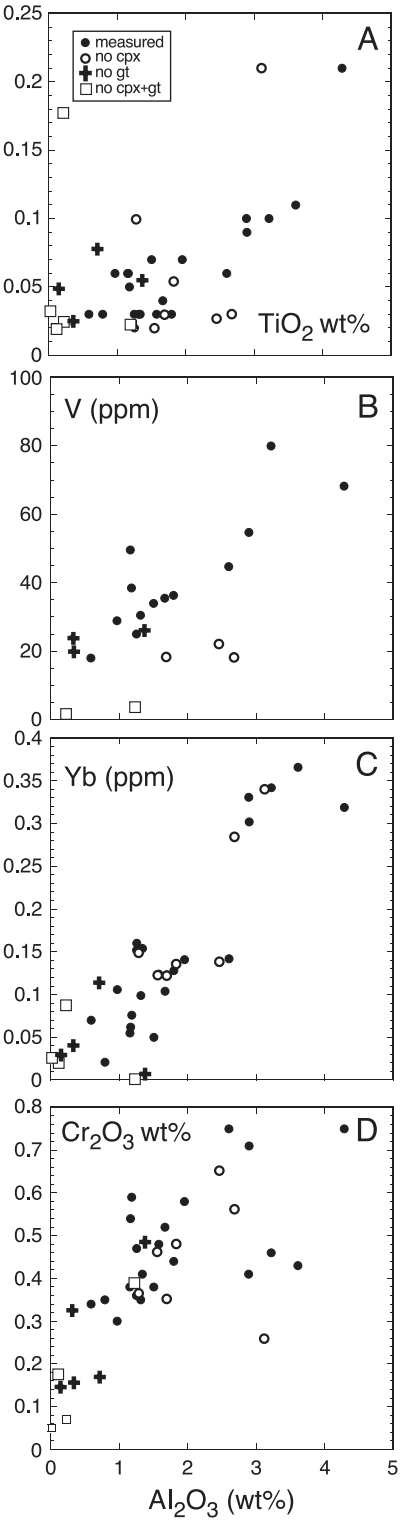

Fig. 6. Abundances of Ti, V, Yb and Cr in cratonic garnet peridotites from Somerset Island, Canada, plotted against Al_2O_3. Shown are the original bulk analyses (measured), and re-calculated whole rock analyses in which clinopyroxene (no cpx), garnet (no gt), and both clinopyroxene and garnet (no cpx + gt), are subtracted from the bulk rock, assuming they were 'introduced' to the residue by metasomatism. The calculations used whole rock, modal and mineral chemical data for large specimens (Schmidberger and Francis, 2001). Note that relative to Al, garnet addition/subtraction does not affect trends for Yb, Sc, Cr and V, whereas clinopyroxene addition/subtraction has a notable affect, but only for V and Ti (the latter element is assumed to behave like Sc). The modeled removal of garnet and clinopyroxene also incorporates the budget for Al.

iour in the mantle. Fig. 6 shows a regular trend for mildly incompatible elements for these samples that could be consistent with simple melt depletion. If it is assumed that clinopyroxene was added to these rocks in a metasomatic process, subtraction of this phase would serve to lower the abundances of only V and Sc (Ti in this example), for a given level of depletion (Al), and would produce far more scatter, compared to the regular depletion trend (Fig. 6A,B). In contrast, subtraction of garnet, if considered to be introduced to these samples, moves samples parallel to the depletion array for all elements, towards lower Al (or level of depletion).

Thus, the effects of clinopyroxene and garnet added by a metasomatic process differ on the mildly incompatible element arrays (Fig. 6). Addition of garnet by metasomatism is indistinguishable from the melt depletion trend, whereas clinopyroxene addition will inflate some element abundances at a constant level of depletion. Relative to Al, significant garnet addition to a peridotite is not substantial for its Yb, Sc, Cr and V contents, whereas clinopyroxene has a notable affect on V and Sc (the latter assumed to behave like Ti). This was also an extreme end-member case because 100% of the garnet and clinopyroxene was assumed to be introduced; as shown above, this is certainly an overestimate for garnet. The 'depletion trends' for mildly incompatible element abundances in peridotites from the database compiled in this study can now be viewed in this light.

5. Element correlations in peridotites

5.1. Cr vs. Al

Covariation of Cr with Al_2O_3 shows essentially no change in Cr content with increasing depletion, irrespective of peridotite sample type or facies. Notable scatter in Cr is generally not present in massif peridotites from outcrop, but restricted to the xenolith and abyssal peridotite data sets. This scatter is ascribed to a 'nugget' effect for spinel. Spinel is a modally minor phase (< 2%) in peridotites but one that dominates the bulk rock budget for Cr. Spinel is adequately sampled in the typically larger specimens of massif peridotites taken in outcrops, but poorly sampled in the smaller xenolith and/or abyssal peridotite specimens (Fig. 7).

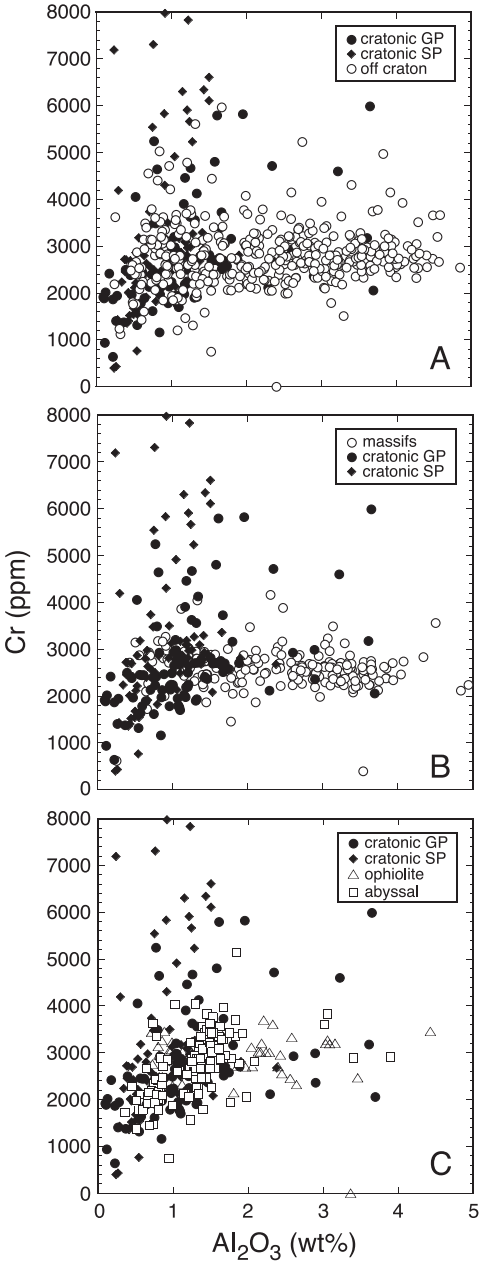

Fig. 7. Cr vs. Al in the world peridotite database comparing (A) on- and off-craton xenoliths (B) cratonic xenoliths and massif peridotites and (C) cratonic xenoliths with abyssal peridotites and ophiolites (Table 2). Note significant scatter in Cr abundances for xenolith specimens, especially at low Al content. SP—spinel peridotite, GP—garnet peridotite.

The latter specimens in the data set are mainly from Ocean Drilling Program shipboard reports where limited sample is permitted for analysis.

Chemical data from peridotite melting experiments show that bulk $D_{Cr/Al}$ between residue/melt decreases substantially with increasing pressure (Fig. 8). In order for Cr to remain constant, and the Cr/Al ratio of a residue to change with depletion, this simple observation from experimental data must require that melting occur mainly at $P<3.0$ GPa where $D_{Cr/Al}$ between melt and residue along the solidus is large. This observation applies to all peridotite samples irrespective of their current pressure of equilibration (i.e., in the garnet- or spinel-facies). Peridotites from both the cratonic data sets (both spinel and garnet bearing), and abyssal spinel peridotites trend to low Cr at less than 2 wt.% Al_2O_3 (Fig. 7C). This trend might suggest that these peridotites formed at P greater than 4 GPa, where $D_{Cr/Al}$ is lower, leaving less Cr in the residue. An origin for abyssal peridotites at greater than 4 GPa can be ruled out on several grounds. The trend of some peridotites to low Cr/Al is most likely due to exhaustion of spinel at high degrees of depletion. Qualitatively, it suggests the garnet-bearing cratonic peridotite samples must have formed in the spinel stability field.

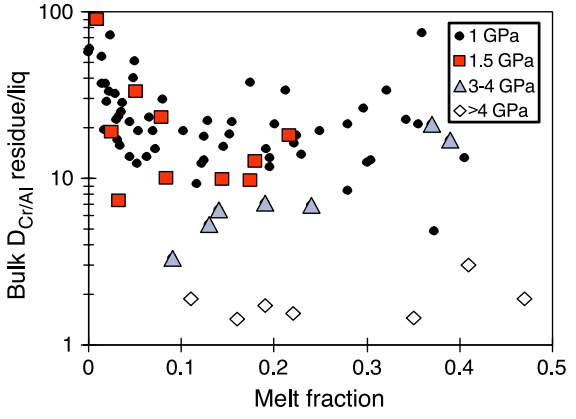

Fig. 8. Compilation of $D_{Cr/Al}$ between bulk residue and melt derived from peridotite melting experiments at various pressures plotted against the degree of partial melting. $D_{Cr/Al}$ is calculated from mass balance of chemical data from the melting experiments (Baker and Stolper, 1994; Falloon et al., 2001; Pickering-Witter and Johnston, 2000; Robinson et al., 1998; Schwab and Johnston, 2001; Walter, 1998). Experiments that did not mass balance for Cr or Al are omitted. Note melting at pressures greater than 3 GPa does not significantly fractionate Cr from Al as is observed in the mantle peridotites (Fig. 7).

5.2. Yb vs. Al

The correlation of Al with Yb in mantle rocks is well known and utilized. The coherency of these two elements in meteorites and their covariation in peridotites has had much utility in estimates of primitive upper mantle (PUM) (Hart and Zindler, 1986; Jagoutz et al., 1979; McDonough and Sun, 1995). These previous studies show a straight line for this array in mantle samples but detailed inspection of samples in this larger database reveals an inflection at ~2 wt.% Al_2O_3 (Fig. 9).

The trend of Yb and Al in residues and its inflection are fit by the melting model only at P of 3 GPa and with the highest D_{Yb} values for all mantle minerals stable at the solidus (Fig. 9). Melting at lower pressure and high D_{Yb} predicts too little Yb in the residue, whereas too much Yb is retained for melting at 7 GPa, even using low D_{Yb} values in the calculations. This trend might suggest that all mantle residues are produced in the garnet stability field but this not the case. At 3 GPa, garnet is not stable in the melting interval of peridotite beyond 10% melting (Robinson and Wood, 1998; Walter, 1998) which corresponds to a residue with only ~3.5% Al_2O_3 (Fig. 2). Most of the melting interval to produce more depleted residues with less than 3 wt.% Al_2O_3 does not involve garnet, but rather clinopyroxene, which plays a major role until its exhaustion at larger degrees of melting (~2 wt.% Al_2O_3—Fig. 2), corresponding almost exactly to the inflection in the Yb–Al array for natural samples (Fig. 9). The match between the inflection derived from the melting model and that in the array of peridotite compositions suggests that the former, although clearly empirical, is a satisfactory description of the residues produced in nature.

Thus, most lithosphere in ophiolites, orogenic massifs and the modern ocean basins (abyssal peridotites) formed at P less than or equal to 3 GPa. Garnet is exhausted with limited melt depletion at this pressure (Fig. 2) and so does not play a major role during melting to form most mantle peridotite residues. Furthermore, the fit of melting model to the residue trend only at high values of

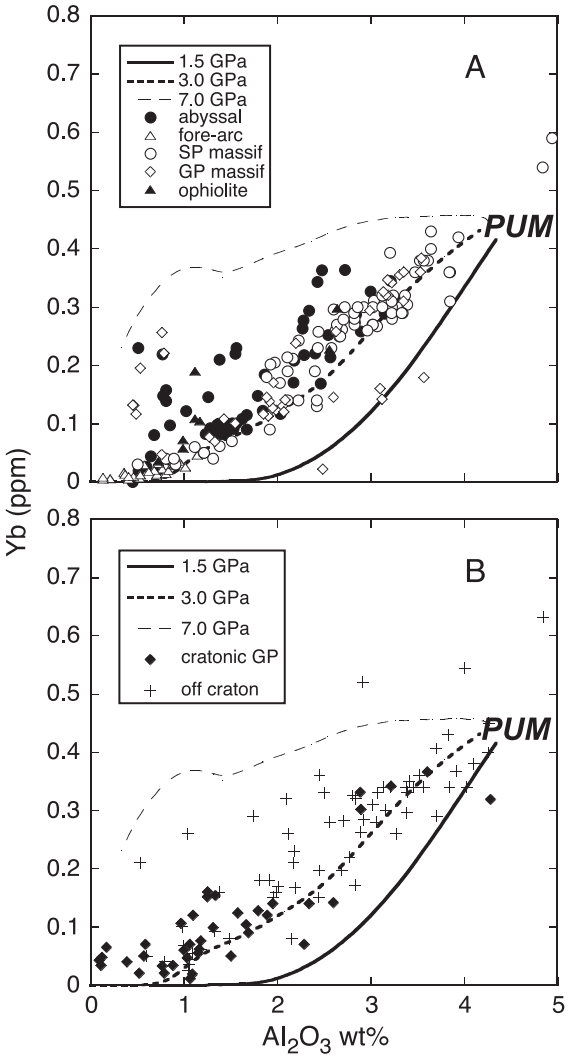

Fig. 9. Covariation of Yb and Al in mantle peridotites. (A) Data for samples from outcrop in 'known' tectonic settings (Table 1). Lines are partial melting trends calculated using a fractional melting model, melting reactions from experiment (see Canil, 2002), and lower limits for D_{Yb} values from Table 2. Higher D_{Yb} values give erratic results. (B) As above but showing cratonic garnet peridotites (GP) and off craton xenolith samples, with same partial melting models as in (A). SP—spinel peridotite, GP—garnet peridotite.

bulk D_{Yb} suggests that Yb and other HREE are quite likely very compatible in near-solidus clinopyroxene, as has been argued on other experimental evidence (Blundy et al., 1998).

The calculated Yb–Al trends can be used to interpret the P of origin of accidental volcanic-hosted xenoliths. All peridotite xenoliths, whether from on- or off-craton, in the garnet or spinel facies, appear to form as residues at P less than 3 GPa (Fig. 9B). Almost no mantle residues plot near the trend exhibited by the 7 GPa melting model. Most interesting is that at a given level of depletion (i.e., Al content), few garnet-bearing mantle samples show the higher Yb expected for residues produced in the garnet stability field because of the large $D_{gt/liq}$ for Yb (Fig. 3). This feature further amplifies the case that garnet is not present during melting to form the residues represented by almost all of the mantle peridotites in this compilation.

5.3. V vs. Al

The behaviour of V during mantle melting is sensitive to fO_2 and variations of this element in peridotite can be a useful paleoredox indicator (Canil and Fedortchouk, 2000). Covariation between V and Al in mantle peridotites has been reviewed (Canil, 2002). Examination of more data for samples from "known" geological environments in this study adds to that analysis. It must be emphasized, however, that the modeling of peridotite V contents in terms of their 'paleoredox' during formation can still only be illustrative because of the pack of internally consistent analytical data for V (Lee et al., 2003).

Abyssal peridotites have the highest V for a given level of depletion and plot along a melting trend consistent with an fO_2 between NNO-2 and NNO-3 (Fig. 10). This fO_2 is identical to that recorded by mid-ocean ridge basalts (Carmichael, 1991) considered to be the complement of abyssal peridotites (Baker and Beckett, 1999). Many abyssal peridotite samples clearly have V in excess of what could be explained by the melting model. It is uncertain whether such samples have experienced V addition (relative to Al) by hydrothermal alteration or impregnation with melt, or have a mantle source with a V content considerably different from PUM. Some of the samples in the database are shipboard measurements requiring relatively small samples, and there may be a bias due to coarse grain sizes.

Mantle tectonites in ophiolites are also interpreted to have formed beneath spreading centers in oceanic

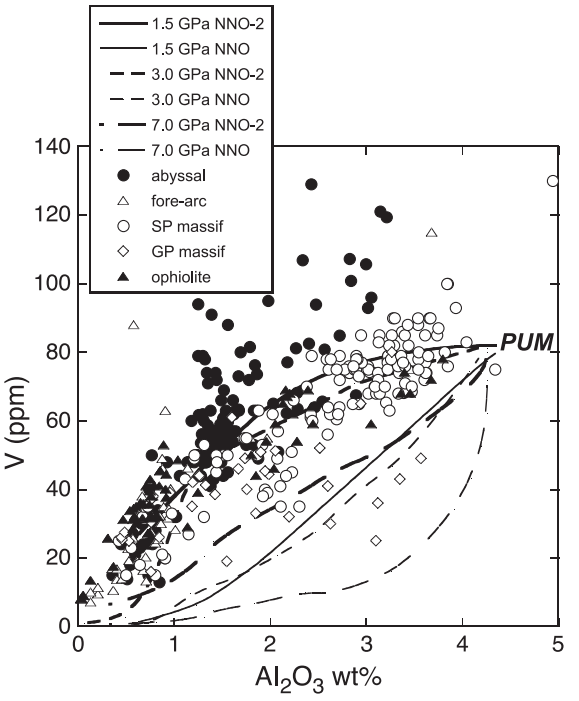

Fig. 10. Covariation of V and Al in mantle peridotites from outcrop in 'known' tectonic settings (Table 2). Comparisons of peridotite compositions with partial melting trends calculated for melting at 1.5, 3.0 and 7.0 GPa and two different log fO_2's relative to the nickel–nickel oxide (NNO) buffer using D_V values from Canil (2002). Note the lack of fit of most residue trends with melting at pressures of 7 GPa, and much better fit between 1.5 and 3 GPa. SP—spinel peridotite, GP—garnet peridotite.

lithosphere, though not necessarily within extensive ocean basins. Ophiolite mantle is slightly less enriched in V when compared to abyssal peridotites, and forms a coherent array along a depletion trend consistent with depletion at a fO_2 similar to that for abyssal peridotites today (Fig. 10). This would suggest that perhaps the scatter to high V contents in many abyssal rocks is a secondary effect.

In contrast, massif peridotites, considered to be sub-continental mantle exhumed in orogenic settings (Den Tex, 1969; Menzies and Dupuy, 1991) form an array with even less V, likely due to melting at higher fO_2 in the continental environment (see also Woodland et al., 1992). There is also no real difference between garnet- or spinel-bearing massif peridotites, though the ultrahigh P garnet peridotites from the Dabie Sulu region form a distinctly low V array (Fig. 10). This has been attributed to formation at very high fO_2 in a convergent margin environment (Canil, 2002). Note from the analysis above that metasomatism in the continental lithosphere would serve to increase the levels of V in the rock at the expense of Al. This means that trends on this diagram require an even higher fO_2 if the rocks had V disturbed by metasomatism.

A large proportion of cratonic peridotite xenoliths form a trend distinct from many other peridotite types. Many of these rocks have low V for a given Al_2O_3 content (Fig. 11). One interpretation is that most cratonic peridotites were formed by melt extraction at a fO_2 higher than that during formation of other types of continental or oceanic mantle lithosphere, perhaps in a convergent margin setting (Canil, 2002). The bulk D_V for melting in the garnet facies is distinctly lower than that in the spinel facies (Canil and Fedortchouk, 2000) and so the low V in many cratonic peridotites could also be equally attributed to higher P of origin. In the absence of other data, it is difficult to separate the effects of P from fO_2 based on

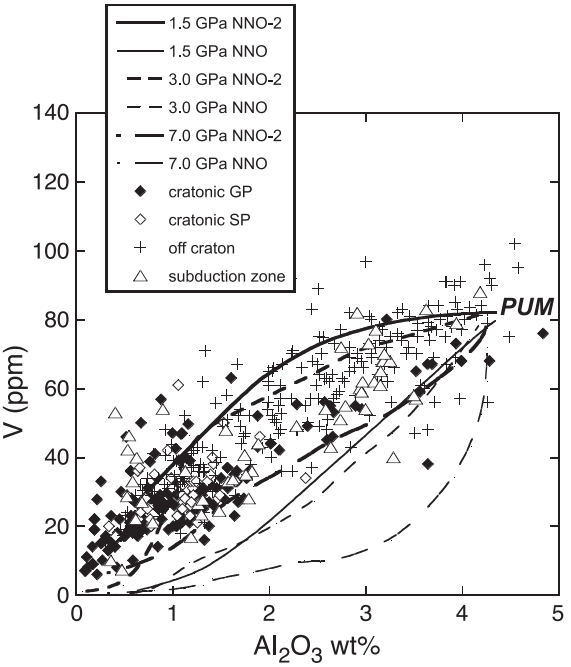

Fig. 11. Covariation of V and Al in mantle peridotites sampled as xenoliths compared with partial melting trends calculated as in Fig. 10. SP—spinel peridotite, GP—garnet peridotite.

V content of cratonic peridotites alone. The covariation of V and Yb, however, can be used to unravel the effect of P versus that of fO_2 in causing the distinct V contents of different types of mantle residues, because Yb is very sensitive to the pressure of melting (Fig. 9).

5.4. V vs. Yb

The Yb–Al covariation in most peridotites is difficult to explain at any P of melting greater than 3 GPa (Fig. 9). This pressure is a maximum, because if the rocks were metasomatized, Yb contents are inflated relative to Al (Fig. 4). Furthermore, the covariation of V and Yb in residues from known geological environments (Fig. 12A) also makes clear that none of the residues from orogenic massifs, ophiolites or abyssal peridotites is consistent with a pressure of melting greater than 3 GPa. The distinctly high V at a given Yb content for abyssal peridotite remains consistent with a lower fO_2 for formation of these peridotites compared to those in ophiolites and massifs.

There is relatively less data for Yb and V in xenoliths, but many cratonic peridotites plot along a distinct array of low V for a given Yb content (Fig. 12B), a distribution similar to that observed in V–Al space (Fig. 11). Thus, it appears that the lower V in these residues is caused by a low bulk D_V during melting at higher fO_2, and pressures below 3 GPa, rather than by melting at higher pressures and lower fO_2.

5.5. Sc vs. Al

Covariations of Sc with Al show an opposite trend than would be predicted by trends with V and Cr. The abyssal peridotite array does not extrapolate to primitive upper mantle values for Sc, but spreads along a distinct trend with high Sc for a given Al content (Fig. 13A). The reasons for this are not presently understood—they may be analytical, or may concern the different behavior of Sc in the mantle than can be modelled here. Alternatively, it is possible the source for abyssal peridotite has a Sc content higher than that in PUM.

The trends for Sc–Al, as well as the inflections at a given degree of depletion in residues are fit by the melting trends at pressures between 1 and 3 GPa and the range of D_{Sc} values encompassed in the experi-

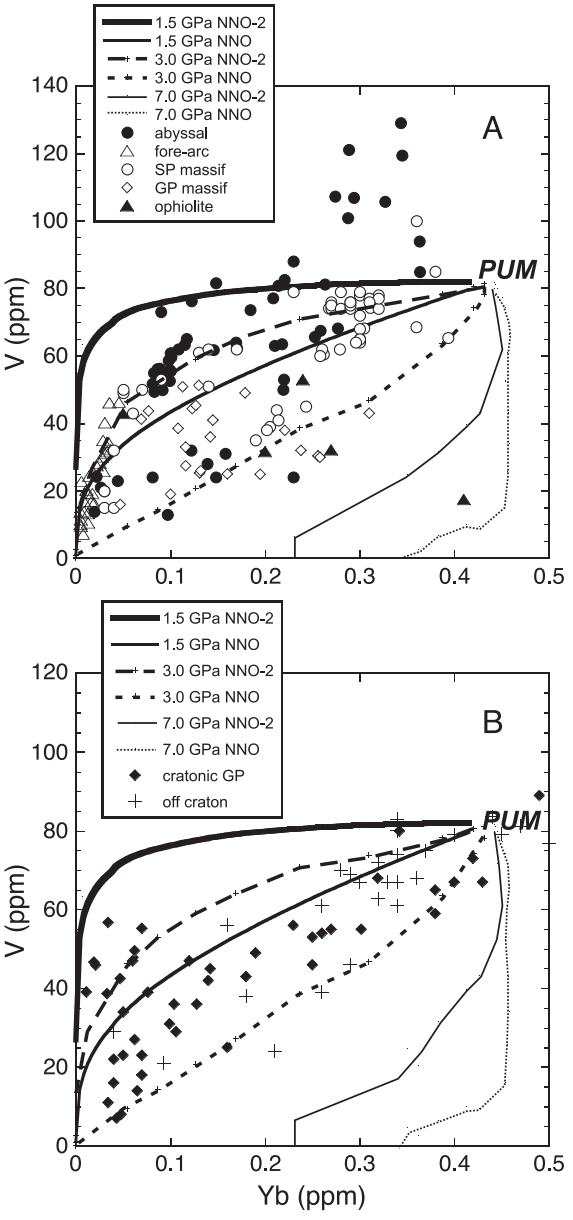

Fig. 12. (A) Covariation of V and Yb in mantle peridotites from outcrop in 'known' tectonic settings (Table 1) compared with partial melting trends calculated for melting at 1.5, 3.0 and 7.0 GPa and two different log fO_2's relative to the nickel–nickel oxide (NNO) buffer using D_V values from Canil (2002) and D_{Yb} from Table 3. (B) As above but comparing melting models with xenolith data. Note the lack of fit of the residue trends with melting at pressures above 3 GPa. SP—spinel peridotite, GP—garnet peridotite.

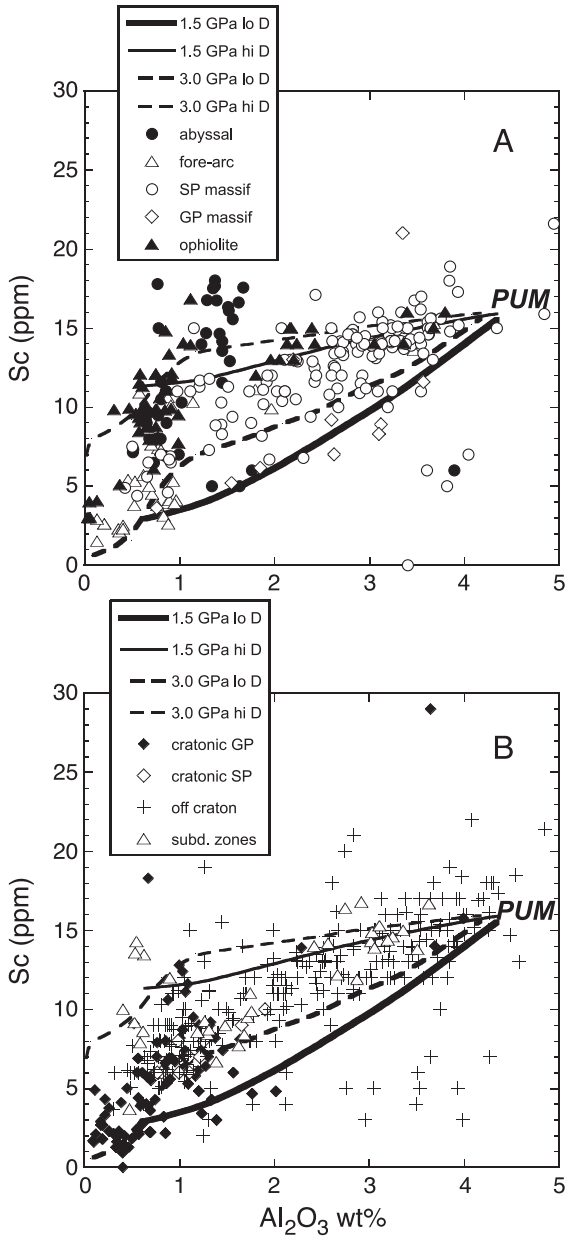

Fig. 13. Covariation of Sc and Al in mantle peridotites from (A) outcrop in 'known' tectonic settings (Table 1), and (B) in xenoliths, compared with partial melting trends calculated for melting at 1.5 and 3.0 GPa using high and low D_{Sc} values from Table 3.

mental measurements. This is especially true for the ophiolite data sets. The xenolith data sets show the same distribution, but there is considerable scatter that may represent an analytical effect (Fig. 13B).

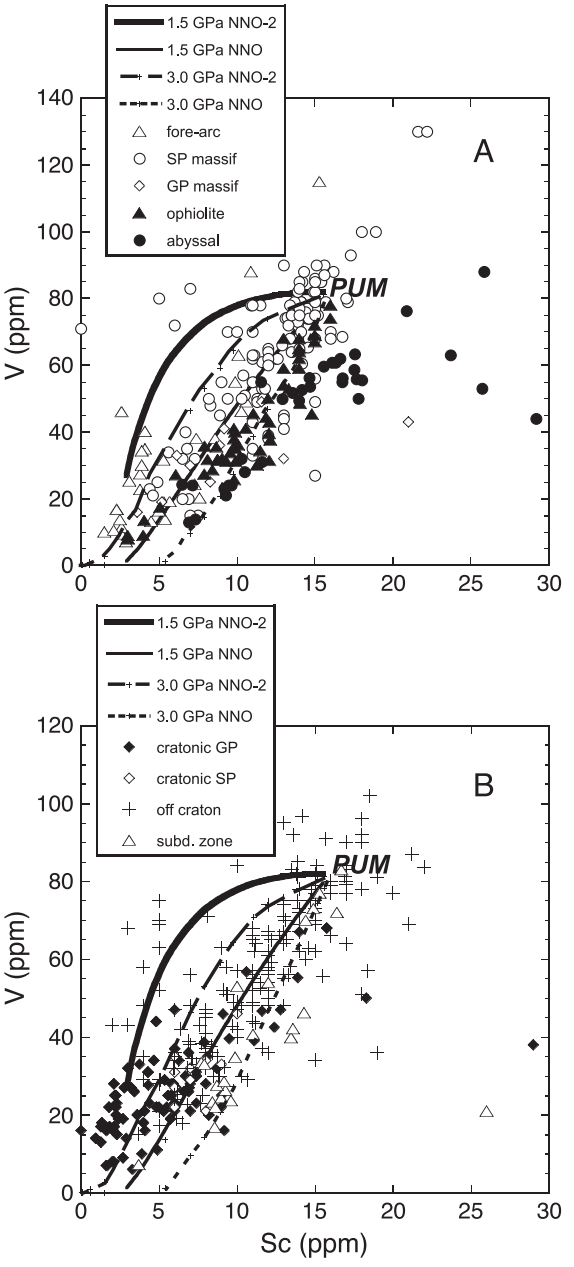

Fig. 14. Covariation of V and Sc in mantle peridotites from (A) outcrop in 'known' tectonic settings (Table 1) and (B) in xenoliths, compared with partial melting trends calculated for melting at 1.5 and 3.0 GPa and two different fO_2's using D_V values from Canil (2002) and low D_{Sc} values from Table 3.

5.6. V vs. Sc

The covariation of these two elements in samples of known geological environment show curious sub-parallel arrays for abyssal, massif and ophiolite-hosted peridotites (Fig. 14A). If it is assumed that Sc behaves similar to Al, then it would appear that abyssal peridotites are low, rather than high in V at a given level of depletion. This is unlikely, because a strong case can be made that V contents are mainly controlled by fO_2 during melting, and that the lower fO_2 of melting at mid-ocean ridges produces the higher V in abyssal peridotites, their complementary residue. The Sc–V trend in abyssal peridotites is perplexing and cannot be explained by any melting model at any reasonable D_{Sc} value (Fig. 14A). One interpretation could be that abyssal peridotites have a mantle source with Sc and V contents that differ from those of PUM. More and better data for the latter samples are required to test this idea.

The xenolith data sets show much scatter, again likely due to analytical effects. A significant number of cratonic peridotites at high levels of depletion have low Sc/V whereas Sc/V increases with level of depletion in abyssal peridotites, ophiolites, and massifs (Fig. 14B). The change in this ratio to low values in the cratonic peridotite data could be due to a detection limit effect in the analyses of these rocks. In most samples from the database, Sc is determined by XRF, which typically has a detection limit for this element near 10 ppm. Because few constraints are offered in publications which report bulk peridotite data, more robust statements cannot be made on the quality of the analytical data for Sc and V.

6. Conclusions

An over-arching observation for all peridotites examined with respect to their Al, Cr, V, Sc and Yb abundances is that almost all mantle peridotites, regardless of sample type (abyssal, orogenic massif, ophiolite, on/off craton xenolith), tectonic environment (divergent margin, convergent margin, passive margin, craton, peri-craton) or the final P of equilibration (plagioclase-, spinel-, or garnet facies) likely originated as lithosphere produced mainly at less than 3 GPa.

Based on whole rock data and residue trends, the original depletion events to form the cratonic mantle lithosphere occurred at lower depths than those at which the mantle was later sampled by kimberlite (> 120 km depth), requiring tectonic transport of lithosphere to these depths beneath the craton, likely by underthrusting, stacking or subduction of originally shallow, spinel-facies residues (Helmstaedt and Schulze, 1989). A similar conclusion has been made on the basis of other evidence (Canil and Wei, 1992; Kelemen et al., 1998; Stachel et al., 1998) and convincing evidence for this process is provided by seismic images of 'frozen subduction' at mantle depths along the western margin of the Archean Slave Province (Bostock, 1998; Cook et al., 1998). In this light, it is difficult to ascribe any large volume of the mantle roots beneath cratons to plume sub-cretion (e.g., Griffin et al., 1999a) or analogous vertical tectonics that arise in plate-less numerical simulations (De Smet et al., 2000). The former models require the generation of residues at pressures far above those required by the melting models using known partitioning of mildly incompatible elements between mantle minerals and melts.

Acknowledgements

This paper is dedicated to F.R. 'Joe' Boyd, a beacon in science. I am grateful to I. Wada, R. Rhodes, J. Thom and P. Leong for entering much of the literature data in this compilation. I also thank C. McCammon, L. Coogan, W. Griffin and H. Grutter for reviews of the paper. This research is supported by a Discovery Grant from NSERC of Canada.

References

Aoki, K., 1981. Major element geochemistry of chromian spinel peridotite xenoliths in the Green Knobs Kimberlite, New Mexico. Sci. Rep. Tohoku Univ., Ser. 3. Mineral. Petrol. Econ. Geol. 1, 127–130.

Aumento, F., Loubat, H., 1971. The Mid-Atlantic ridge near 45 degrees N; XVI, Serpentinized ultramafic intrusions. Can. J. Earth Sci. 8, 631–633.

Baker, M.B., Beckett, J.R., 1999. The origin of abyssal peridotites,

a reinterpretation of constraints based on primary bulk compositions. Earth Planet. Sci. Lett. 171, 49–61.
Baker, M.B., Stolper, E.M., 1994. Determining the composition of high-pressure mantle melts using diamond aggregates. Geochim. Cosmochim. Acta 58, 2811–2827.
Beattie, P., 1994. Systematics and energetics of trace element partitioning between olivine and silicate melts: implications for the nature of mineral/melt partitioning. Chem. Geol. 117, 57–71.
Becker, H., 1996. Geochemistry of garnet peridotite massifs from lower Austria and the composition of deep lithosphere beneath a Palaeozoic convergent plate margin. Chem. Geol. 134, 49–65.
Bedini, R.M., Bodinier, J.-L., Dautria, J.-M., Morten, L., 1997. Evolution of LILE-enriched small melt fractions in the lithospheric mantle: a case study from the East African Rift. Earth Planet. Sci. Lett. 153, 67–83.
Bernstein, S., Kelemen, P.B., Brooks, C.K., 1998. Depleted spinel harzburgite xenoliths in Tertiary dykes from East Greenland: Restites from high degree melting. Earth Planet. Sci. Lett. 154, 221–235.
Berry, R.F., 1981. Petrology of the Hili Manu lherzolite, East Timor. J. Geol. Soc. Aust. 28, 453–469.
Blundy, J.D., Robinson, J.A.C., Wood, B.J., 1998. Heavy REE are compatible in clinopyroxene on the spinel lherzolite solidus. Earth Planet. Sci. Lett. 160, 493–504.
Bodinier, J.L., 1988. Geochemistry and petrogenesis of the Lanzo peridotite body, Western Alps. Tectonophysics 149, 67–88.
Bodinier, J.L., Dupuy, C., Dostal, J., 1988. Geochemistry and petrogenesis of Eastern Pyrenean peridotites. Geochim. Cosmochim. Acta 52, 2893–2907.
Bonatti, E., Ottonello, G., Hamlyn, P.R., 1986. Peridotites from the island of Zabargad (St. John), Red Sea: petrology and geochemistry. J. Geophys. Res. 91, 599–631.
Bostock, M.G., 1998. Mantle stratigraphy and evolution of the Slave province. J. Geophys. Res. 103, 21183–21200.
Boyd, F.R., 1999. Spinel-facies peridotites from the Kaapvaal root. In: Gurney, J. (Ed.), Proc. 7th Inter. Kimb. Conf.. Red Roof Designs, Capetown, pp. 40–48.
Boyd, F.R., Mertzman, S.A., 1987. Composition and structure of the Kaapvaal lithosphere, southern Africa. In: Mysen, B.O. (Ed.), Magmatic Processes, Physicochemical Principles. Geochemical Society, Washington, DC, pp. 13–24.
Boyd, F.R., Nixon, P.H., Pearson, D.G., Mertzman, S.A., 1993. Low-calcium garnet harzburgites from southern Africa: their relations to craton structure and diamond crystallization. Contrib. Mineral. Petrol. 113, 352–366.
Boyd, F.R., et al., 1997. Composition of the Siberian cratonic mantle: evidence from Udachnaya peridotite xenoliths. Contrib. Mineral. Petrol. 128, 228–246.
Brandon, A.D., Snow, J.E., Walker, R.J., Morgan, J.W., Mock, T.D., 2000. 190Pt–186Os and 187Re–187Os systematics of abyssal peridotites. Earth Planet. Sci. Lett. 177, 319–335.
Burnham, O., Rogers, N.W., Pearson, D.G., van Calsteren, P.W., Hawkesworth, C.J., 1998. The petrogenesis of the eastern Pyrenean peridotites: An integrated study of their whole rock geochemistry and Re–Os isotope composition. Geochim. Cosmochim. Acta 62, 2293–2310.
Canil, D., 1991. Experimental evidence for the exsolution of cratonic peridotite from high-temperature harzburgite. Earth Planet. Sci. Lett. 106, 64–72.
Canil, D., 1992. Orthopyroxene stability along the peridotite solidus and the origin of cratonic lithosphere beneath southern Africa. Earth Planet. Sci. Lett. 111, 83–95.
Canil, D., 1999. The Ni-in-garnet geothermometer: calibration at natural abundances. Contrib. Mineral. Petrol. 136, 240–246.
Canil, D., 2002. Vanadium in peridotites, mantle redox and tectonic environments: Archean to present. Earth Planet. Sci. Lett. 195, 75–90.
Canil, D., Fedortchouk, Y., 2000. Clinopyroxene–liquid partitioning for vanadium and the oxygen fugacity during formation of cratonic and oceanic mantle lithosphere. J. Geophys. Res. 105, 26003–26016.
Canil, D., Fedortchouk, Y., 2001. Olivine–liquid partitioning of vanadium and other trace elements, with applications to ancient and modern picrites. Can. Mineral. 39, 319–330.
Canil, D., Wei, K., 1992. Constraints on the origin of mantle-derived low Ca garnets. Contrib. Mineral. Petrol. 109, 421–430.
Canil, D., Johnston, S.T., Evers, K., Shellnutt, J.G., Creaser, R.C., 2003. Mantle exhumation in an early Paleozoic passive margin, northern Cordillera, Yukon. J. Geol. 111, 313–327.
Carlson, R., Irving, A.J., Hearn Jr., B.C. 1999. Peridotites of the Wyoming craton. In: Gurney, J. (Ed.), Proc. 7th Inter. Kimb. Conf. Red Roof Designs, Capetown, pp. 440–448.
Carmichael, I.S.E., 1991. The redox states of basic and silicic magmas: a reflection of their source regions? Contrib. Mineral. Petrol. 106, 129–141.
Casey, J.F., 1997. Comparison of major and trace-element geochemistry of abyssal peridotites and mafic plutonics with basalts from the MARK region of the Mid-Atlantic Ridge. In: Karson, J.A., Cannat, M., Miller, D.J., et al. (Eds.), Proc. Sci. Results ODP Leg, vol. 153. Ocean Drilling Program, College station, Texas, pp. 181–241.
Chauvel, C., Jahn, B.M., 1984. Nd–Sr isotope and REE geochemistry of alkali basalts from the Massif Central, France. Geochim. Cosmochim. Acta 48, 93–110.
Coogan, L., et al. Abyssal peridotites and basalts along a flow line from the southwest Indian Ridge. Chem. Geol., in press.
Cook, F.A., van der Velden, A.J., Hall, K.W., Roberts, B.J., 1998. Tectonic delamination and subcrustal imbrication of the Precambrian lithosphere in northwestern Canada mapped by LITHOPROBE. Geology 26, 839–842.
Cox, K.G., Smith, M.R., Beswetherick, S., 1987. Textural studies of garnet lherzolites: evidence of exsolution origin from high-temperature harzburgites. In: Nixon, P.H. (Ed.), Mantle Xenoliths. Wiley, Chichester, pp. 537–550.
Dautria, J.M., Girod, M., 1986. Les enclaves de lherzolite a spinelle et plagioclase du volcan DeDibi (Adamoua, Camerou):des temoins d'un manteau superieur anormal. Bull. Mineral. 109, 275–288.
Dautria, J.M., Dupuy, C., Takherist, D., Dostal, J., 1992. Carbonate metasomatism in the lithospheric mantle: peridotitic xenoliths from a melilitic district of the Sahara basin. Contrib. Mineral. Petrol. 111, 37–52.
Den Tex, E., 1969. Origin of ultramafic rocks, their tectonic setting

and history: a contribution to the discussion of the paper "The origin of ultramafic and ultrabasic rocks" by P.J. Wyllie. Tectonophysics 7, 457–488.

De Smet, J., Van den Berg, A.P., Vlaar, N.J., 2000. Early formation and long-term stability of continents resulting from decompression melting in a convecting mantle. Tectonophysics 322, 19–33.

Dupuy, C., Dostal, J., Bodinier, J.L., 1987. Geochemistry of spinel peridotite inclusions in basalts from Sardinia. Mineral. Mag. 51, 561–568.

Ehrenberg, S.N., 1982. Petrogenesis of garnet lherzolite and megacrystalline nodules from the Thumb, Navajo volcanic field. J. Petrol. 23, 505–545.

Embey-Isztin, A., Scharbert, H.G., Dietrich, H., Poultidis, H., 1989. Petrology and geochemistry of peridotite xenoliths in alkali basalts from the Transdanubian volcanic region, west Hungary. J. Petrol. 30, 79–105.

Ernst, W.G., 1978. Petrochemical study of lherzolitic rocks from the Western Alps. J. Petrol. 19, 341–392.

Fabries, J., Lorand, J.P., Bodinier, J.L., Dupuy, C., 1991. Evolution of the upper mantle beneath the Pyrenees: evidence from orogenic spinel lherzolite massifs. J. Petrol., 55–76 (Spec. Lherzolites Issues).

Falloon, T.J., Danyushevsky, L.V., Green, D.H., 2001. Peridotite melting at 1 GPa: reversal experiments on partial melt compositions produced by peridotite–basalt sandwich experiments. J. Petrol. 42, 2363–2390.

Francis, D., 1987. Mantle–melt interaction recorded in spinel lherzolite xenoliths from the Alligator Lake volcanic complex, Yukon, Canada. J. Petrol. 28, 569–597.

Franz, L., Becker, K.-P., Kramer, W., Herzig, P.M., 2002. Metasomatic mantle xenoliths from the Bismarck microplate (Papua New Guinea)—Thermal evolution, geochemistry and extent of slab-induced metasomatism. J. Petrol. 43, 315–343.

Frey, F.A., Green, D.H., 1974. The mineralogy, geochemistry and origin of lherzolite inclusions in Victorian basanites. Geochim. Cosmochim. Acta 38, 1023–1059.

Frey, F.A., Suen, C.J., Stockman, H.W., 1985. The Ronda high temperature peridotite: geochemistry and petrogenesis. Geochim. Cosmochim. Acta 49, 2469–2491.

Gaetani, G.A., Grove, T.L., 1995. Partitioning of rare earth elements between clinopyroxene and silicate melt: crystal chemical controls. Geochim. Cosmochim. Acta 59, 1951–1962.

Gillis, K., Mevel, C., Allan, J., et al., 1993. Initial Reports-Proceedings of Ocean Drilling Program Hess Deep, vol. 147. Ocean Drilling Program, College Station, Texas, pp. 1–29.

Glaser, S., Foley, S.F., Gunther, D., 1999. Trace element compositions of minerals in garnet and spinel peridotite xenoliths from the Vitim volcanic field, Transbaikalia, eastern Siberia. Lithos 48, 263–285.

Gregoire, M., Moine, B.N., O'Reilly, S.Y., Cottin, J.Y., Giret, A., 2000. Trace element residence and partitioning in mantle xenoliths metasomatized by highly alkaline, silicate- and carbonate-rich melts (Kerguelen Islands, Indian Ocean). J. Petrol. 41, 477–509.

Griffin, W.L., Sutherland, F.L., Hollis, J.D., 1987. Geothermal profile and crust–mantle transition beneath east-central Queensland: volcanology, xenolith petrology and seismic data. J. Volcanol. Geotherm. Res. 31, 177–203.

Griffin, W.L., O'Reilly, S.Y., Ryan, C.G., 1999a. The composition and origin of sub-continental lithospheric mantle. In: Fei, Y., Bertka, C.M., Mysen, B.O. (Eds.), Mantle Petrology, Field Observations and High Pressure Experimentation. The Geochemical Society, Washington, DC.

Griffin, W.L., Shee, S.R., Ryan, C.G., Win, T.T., Wyatt, B.A., 1999b. Harzburgite to lherzolite and back again: metasomatic processes in ultramafic xenoliths from the Wesselton kimberlite, Kimberley, South Africa. Contrib. Mineral. Petrol. 134, 232–250.

Gruau, G., Lecuyer, C., Bernard-Griffiths, J., Morin, N., 1991. Origin and petrogenesis of the Trinity Ophiolite Complex (California): new constraints from REE and Nd isotope data. J. Petrol., 229–242 (Spec. Lherz. Issue).

Gruau, G., Bernard-Griffiths, J., Lecuyer, C., 1998. The origin of U-shaped rare earth patterns in ophiolite peridotites: assessing the role of secondary alteration and melt/rock reaction. Geochim. Cosmochim. Acta 62, 3545–3560.

Gueddari, K., Piboule, M., Amossé, J., 1996. Differentiation of platinum-group elements (PGE) and of gold during partial melting of peridotites in the lherzolitic massifs of the Betico-Rifean range (Ronda and Beni Bousera). Chem. Geol. 134, 181–197.

Hart, S.R., Dunn, T., 1993. Experimental cpx/melt partitioning of 24 trace elements. Contrib. Mineral. Petrol. 113, 1–8.

Hart, S.R., Zindler, A., 1986. In search of a bulk earth composition. Chem. Geol. 57, 247–267.

Hartmann, G.H., Wedepohl, K.H., 1993. The composition of peridotite tectonites from the Ivrea Complex, northern Italy: residues of melt extraction. Geochim. Cosmochim. Acta 57, 1761–1782.

Hauri, E., Shimizu, N., Dieu, J.J., Hart, S.R., 1993. Evidence for hotspot-related carbonatite metasomatism in the oceanic upper mantle. Nature 365, 221–227.

Hauri, E.H., Wagner, T., Grove, T.L., 1994. Experimental and natural partitioning of Th, U, Pb and other trace elements between garnet, clinopyroxene and basaltic. Chem. Geol. 117, 149–166.

Helmstaedt, H., Schulze, D.J., 1989. Southern African kimberlites and their mantle sample: implications for the Archaean tectonics and lithosphere evolution. Spec. Publ.-Geol. Soc. Aust. 14, 358–368.

Herzberg, C.H., 1995. Generation of plume magmas through time: an experimental perspective. Chem. Geol. 126, 1–16.

Horn, I., Foley, S.F., Jackson, S.E., Jenner, G.A., 1994. Experimentally determined partitioning of high field strength and selected transition elements between spinel and basaltic melt. Chem. Geol. 117, 193–218.

Hunter, R.H., Upton, B.G.J., 1987. The British Isles—A Paleozoic mantle sample. In: Nixon, P.H.N. (Ed.), Mantle Xenoliths. Wiley, New York, pp. 107–118.

Ionov, D., Ashchepkov, I.V., Stosch, H.-G., Witt-Eickschen, G., Seck, H.A., 1993. Garnet peridotite xenoliths from the Vitim volcanic field, Baikal region: the nature of the garnet–spinel peridotite transition zone in the continental mantle. J. Petrol. 34, 1141–1175.

Jagoutz, E., et al., 1979. The abundances of major, minor and trace elements in the earth's mantle as derived from primitive ultramafic nodules. 10th Lunar and Planetary Science Conference. NASA, Houston, TX, pp. 2031–2050.

Jaques, A.L., Chappell, B.W., 1980. Petrology and trace element geochemistry of the Papuan Ultramafic belt. Contrib. Mineral. Petrol. 75, 55–70.

Jaques, A.L., O'Neill, H.S.C., Smith, C.B., Moon, J., Chappell, B.W., 1990. Diamondiferous peridotite xenoliths from the Argyle (AK1) lamproite pipe, western Australia. Contrib. Mineral. Petrol. 104, 255–276.

Johnson, K.T.M., 1998. Experimental determination of partition coefficients for rare earth and high-field strength elements between clinopyroxene, garnet and basaltic melt at high pressures. Contrib. Mineral. Petrol. 133, 60–68.

Johnson, K.T.M., Dick, H.J.B., Shimizu, N., 1990. Melting in the oceanic upper mantle: an ion microprobe study of diopsides in abyssal peridotites. J. Geophys. Res. 95, 2661–2678.

Jordan, T.H., 1975. The continental tectosphere. Rev. Geophys. Space Phys. 13, 1–12.

Kelemen, P.B., Hart, S.R., Bernstein, S., 1998. Silica enrichment in the continental upper mantle via melt/rock reaction. Earth Planet. Sci. Lett. 164, 387–406.

Kennedy, A.K., Lofgren, G.E., Wasserburg, G.J., 1992. An experimental study of trace element partitioning between olivine, orthopyroxene and melt in chondrules: equilibrium values and kinetic effects. Earth Planet. Sci. Lett. 115, 177–195.

Kopylova, M., Russell, J.K., 2000. Chemical stratification of cratonic lithosphere: constraints from the northern Slave craton, Canada. Earth Planet. Sci. Lett. 181, 71–87.

Laurora, A., et al., 2001. Metasomatism and melting in carbonated peridotite xenoliths from the mantle wedge: the Gobernador Gregores Case (southern Patagonia). J. Petrol. 42, 69–87.

Lee, C.-T., Rudnick, R.L., 1999. Compositionally stratified cratonic lithosphere: petrology and geochemistry of peridotite xenoliths from the Labait volcano, Tanzania. 7th International Kimberlite Conference. Red Roof Designs, Capetown, pp. 503–521.

Lee, C.T., Brandon, A., Norman, M.D., 2003. Vanadium as a proxy for paleo-fO2 during partial melting: prospects, limitations and implications. Geochim. Cosmochim. Acta 67, 3045–3064.

Lenoir, X., Garrido, C.J., Bodinier, J.-L., Dautria, J.-M., 2000. Contrasting lithospheric mantle domains beneath the Massif Central (France) revealed by geochemistry of peridotite xenoliths. Earth Planet. Sci. Lett. 181, 359–375.

Lenoir, X., Garrido, C.J., Bodinier, J.-L., Dautria, J.-M., Gervilla, F., 2001. The recrystallization front of the Ronda Peridotite: evidence for melting and thermal erosion of subcontinental lithospheric mantle beneath the Alboran Basin. J. Petrol. 42, 141–158.

Liang, Y., Elthon, D., 1990. Geochemistry and petrology of spinel lherzolite xenoliths from Xalapasco de La Joya, San Luis Potosi, Mexico, Partial melting and mantle metasomatism. J. Geophys. Res. 95, 15859–15878.

Loney, R.A., Himmelberg, G.R., Coleman, R.G., 1971. Structure and petrology of the Alpine-type peridotite at Burro Mountain, California, USA. J. Petrol. 12, 245–310.

Luhr, J.F., Aranda-Gomez, J.J., 1997. Mexican peridotite xenoliths and tectonic terranes: correlations among vent location, texture, temperature, pressure, and oxygen fugacity. J. Petrol. 38, 1075–1112.

Maaloe, S., Aoki, K., 1977. The major element composition of the upper mantle estimated from the composition of lherzolites. Contrib. Mineral. Petrol. 63, 161–173.

Maury, R., Defant, M., Joron, J.-L., 1992. Metasomatism of the sub-arc mantle inferred from trace elements in Philippine xenoliths. Nature 360, 661–663.

McDonough, W.F., Sun, S.S., 1995. The composition of the earth. Chem. Geol. 120, 223–253.

McInnes, B.I.A., Gregoire, M., Binns, R.A., Herzig, P.M., Hannington, M.D., 2001. Hydrous metasomatism of oceanic sub-arc mantle, Lihir, Papua New Guinea: petrology and geochemistry of fluid-metasomatised mantle wedge xenoliths. Earth Planet. Sci. Lett. 188, 169–183.

McKenzie, D., O'Nions, R.K., 1991. Partial melt distributions from inversion of rare earth element concentrations. J. Petrol. 32, 1021–1092.

McPherson, E., Thirlwall, M.F., Parkinson, I.J., Menzies, M.A., Bodinier, J.L., Woodland, A., Bussod, G., 1996. Geochemistry of metasomatism adjacent to amphibole-bearing veins in the Lherz peridotite massif. Chem. Geol. 134, 135–157.

Menzies, M.A., Hawkesworth, C.J., 1987. Upper mantle processes and composition. In: Nixon, P.H.N. (Ed.), Mantle Xenoliths. Wiley, New York, pp. 725–738.

Menzies, M., Dupuy, C., 1991. Orogenic massifs: protolith, process and provenance. J. Petrol., 1–16 (Spec. Lherzolites Issues).

Miyashiro, A., Shido, F., Ewing, M., 1969. Composition and origin of serpentinites from the mid-Atlantic Ridge near 24° and 30° north latitude. Contrib. Mineral. Petrol. 23, 117–127.

Morten, L., 1987. Italy: a review of xenolithic occurrences and their comparison with Alpine peridotites. In: Nixon, P.H. (Ed.), Mantle Xenoliths. Wiley, New York, pp. 135–148.

Nagasawa, H., Schreiber, H.D., Morris, R.V., 1980. Experimental mineral/liquid partition coefficients of the rare Earth elements, Sc and Sr for perovskite, spinel and melilite. Earth Planet. Sci. Lett. 46, 431–437.

Niu, Y., Hekinian, R., 1997. Basaltic liquids and harzburgitic residues in the Garrett Transform: a case study at fast spreading ridges. Earth Planet. Sci. Lett. 146, 243–258.

Palme, H., Nickel, K., 1985. Ca/Al ratio and composition of the Earth's mantle. Geochim. Cosmochim. Acta 49, 2123–2132.

Parkinson, I.J., Pearce, J.A., 1998. Peridotites from the Izu-Bonin-Mariana Forearc (ODP Leg 125): evidence for mantle melting and melt–mantle interaction in a supra-subduction zone setting. J. Petrol. 39, 1577–1618.

Pearce, J.A., Barker, P.F., Edwards, S.J., Parkinson, I.J., Leat, P.T., 2000. Geochemistry and tectonic significance of peridotites from the South Sandwich arc-basin system, South Atlantic. Contrib. Mineral. Petrol. 139, 36–53.

Pearson, D.G., Irvine, G.J., Carlson, R.W., Kopylova, M.G., Ionov, D.A., 2002. The development of lithospheric keels beneath the earliest continents: time constraints using PGE and Re–Os isotope systematics. In: Fowler, C.M.R., Ebinger, C.J., Hawkesworth, C.J. (Eds.), The Early Earth Physical, Chemical and

Biological Development. Spec. Publ.-Geol. Soc. London, vol. 199, pp. 65–90.

Pearson, D.G., Canil, D., Shirey, S.B., 2003. Mantle samples included in volcanic rocks: xenoliths and diamonds. In: Carlson, R.W. (Ed.), Treatise in Geochemistry, vol. 2. Elsevier, Amsterdam, pp. 171–276.

Peltonen, P., Huhma, H., Tyni, M., Shimizu, N., 1999. Garnet peridotite xenoliths from kimberlites of Finland: nature of the continental mantle at an Archean craton–Proterozoic mobile belt transition. In: Gurney, J. (Ed.), Proc. 7th Int. Kimb. Conf. Red Roof Designs, Capetown, pp. 664–670.

Peslier, A.H., Francis, D., Ludden, J., 2002. The lithospheric mantle beneath continental margins: melting and melt–rock reaction in Canadian Cordillera Xenoliths. J. Petrol. 43, 2013–2047.

Pickering-Witter, J., Johnston, A.D., 2000. The effects of variable bulk composition on the melting systematics of fertile peridotitic assemblages. Contrib. Mineral. Petrol. 140, 190–211.

Poudjom Djomani, Y.H., O'Reilly, S.Y., Griffin, W.L., Morgan, P., 2001. The density structure of subcontinental lithosphere through time. Earth Planet. Sci. Lett. 184, 605–621.

Press, S., Witt, G., Seck, H.A., Eonov, D., Kovalenko, V.I., 1986. Spinel peridotite xenoliths from the Tariat Depression, Mongolia: II. Geochemistry and Nd and Sr isotopic composition and their implications for the evolution of the subcontinental lithosphere. Geochim. Cosmochim. Acta 50, 2587–2599.

Prinz, M., et al., 1976. Ultramafic and mafic dredge samples from the equatorial Mid-Atlantic Ridge and fracture zones. J. Geophys. Res. 81, 4087–4103.

Qi, Q., Taylor, L.A., Zhou, X., 1995. Petrology and geochemistry of mantle peridotite xenoliths from SE China. J. Petrol. 36, 55–79.

Rampone, E., Piccardo, G.B., Vannucci, R., Bottazzi, P., Ottoline, L., 1993. Subsolidus reactions monitored by trace element partitioning: the spinel- to plagioclase-facies transition in mantle peridotes. Contrib. Mineral. Petrol. 115, 1–17.

Rampone, E., et al., 1996. Trace element and isotope geochemistry of depleted peridotites from an N-MORB type ophiolite (internal Liguride, N. Italy). Contrib. Mineral. Petrol. 123, 61–76.

Robinson, J.A.C., Wood, B.J., 1998. The depth of the spinel to garnet transition at the peridotite solidus. Earth Planet. Sci. Lett. 164, 277–284.

Robinson, J.A.C., Wood, B.J., Blundy, J.D., 1998. The beginning of melting of fertile and depleted peridotite at 1.5 GPa. Earth Planet. Sci. Lett. 155, 97–111.

Rudnick, R.J., McDonough, W.F., Chappell, B.W., 1993. Carbonatite metasomatism in the northern Tanzanian mantle: petrographic and geochemical characteristics. Earth Planet. Sci. Lett. 114, 463–475.

Scambelluri, M., Rampone, E., Piccardo, G., 2001. Fluid and element cycling in subducted serpentinite: a trace-element study of the Erro–Tobbio High-Pressure Ultramafites (Western Alps, NW Italy). J. Petrol. 42, 55–67.

Schmidberger, S.S., Francis, D., 2001. Constraints on the trace element composition of the Archean mantle root beneath Somerset Island, Arctic Canada. J. Petrol. 42, 1095–1117.

Schwab, B.E., Johnston, A.D., 2001. Melting systematics of modally variable, compositionally intermediate peridotites and effects of mineral fertility. J. Petrol. 42, 1789–1811.

Schwandt, C., McKay, G.A., 1998. Rare earth element partition coefficients from enstatite/melt synthesis experiments. Geochim. Cosmochim. Acta 62, 2845–2848.

Seifert, K., Brunotte, D., 1996. Geochemistry of serpentinized mantle peridotite from Site 897 in the Iberia Abyssal Plain. Proc. Ocean Drill. Program Sci. Result 149, 143.

Shervais, J.W., Mukasa, S.B., 1991. The Balmuccia orogenic lherzolite massif, Italy. Journal of Petrology, 155–174 (Special issue).

Shi, L., Francis, D., Ludden, J., Frederiksen, A., Bostock, M., 1998. Xenolith evidence for lithospheric melting above anomalously hot mantle under the northern Canadian Cordillera. Contrib. Mineral. Petrol. 131, 39–53.

Shimizu, N., Sobolev, N.V., Yefimova, E.S., 1997. Chemical heterogeneities of inclusion garnets and juvenile character of peridotitic diamonds from Siberia. Russ. Geol. Geophys. 38, 356–372.

Siena, F., Beccaluva, L., Coltorti, M., Marchesi, S., Morra, V., 1991. Ridge to Hot-spot evolution of the Atlantic lithospheric mantle: evidence from Lanzarote peridotite xenoliths (Canary Islands). J. Petrol., 269–289 (Special Lherzolites Issue).

Simon, N.S.C., Irvine, G.J., Davies, G.R., Pearson, D.G., Carlson, R.W., 2003. The origin of garnet and clinopyroxene in "depleted" Kaapvaal peridotites. Lithos 71, 289–322.

Smith, D., Boyd, F.R., 1992. Compositional zonation in garnets of peridotite xenoliths. Contrib. Mineral. Petrol. 112, 134–147.

Smith, D., Levy, S., 1976. Petrology of Green Knobs diatreme, New Mexico, and implications for the mantle below the Colorado Plateau. Earth Planet. Sci. Lett. 19, 107–125.

Smith, D., Griffin, W.L., Ryan, C.G., Sie, S.H., 1991. Trace-element zonation in garnets from The Thumb: heating and melt infiltration below the Colorado Plateau. Contrib. Mineral. Petrol. 107, 60–79.

Smith, D., Riter, J.C.A., Mertzman, S.A., 1999. Water rock interactions, orthopyroxene growth and Si-enrichment in the mantle: evidence in xenoliths from the Colorado Plateau, southwestern United States. Earth Planet. Sci. Lett. 167, 347–356.

Snow, J.E., Dick, H.J.B., 1995. Pervasive magnesium loss by marine weathering of peridotite. Geochim. Cosmochim. Acta 59, 4219–4235.

Song, Y., Frey, F.A., 1989. Geochemistry of peridotite xenoliths in basalt from Hannuoba, eastern China: Implications for subcontinental mantle heterogeneity. Geochim. Cosmochim. Acta 53, 97–113.

Stachel, T., Viljoen, K.S., Brey, G., Harris, J.W., 1998. Metasomatic processes in lherzolitic and harzburgitic domains of diamondiferous lithospheric mantle: REE in garnets from xenoliths and inclusions in diamonds. Earth Planet. Sci. Lett. 159, 1–12.

Stephens, C.J., 1997. Heterogeneity of oceanic peridotite from the western canyon wall at MARK: results from Site 920. In: Karson, J.A., Cannat, M., Miller, D.J., Elthon, D. (Eds.), Proc. Ocean Drill. Program Sci. Results Leg, vol. 153. Ocean Drilling Program, College station, Texas, pp. 233–285.

Stolz, A.J., Davies, G.R., 1991. Chemical and isotopic evidence from spinel lherzolite xenoliths for episodic metasomatism of the upper mantle beneath southeastern Australia. J. Petrol., 303–330 (Special Volume, Special Lherzolites Issue).

Takazawa, E., Frey, F.A., Shimizu, N., Obata, M., 2000. Whole

rock compositional variations in an upper mantle peridotite (Horoman, Hokkaido, Japan): are they consistent with a partial melting process? Geochim. Cosmochim. Acta 64 (4), 695–716.

Ulmer, P., 1989. Partitioning of high field strength elements among olivine, pyroxenes, garnet and calc-alkaline picrobasalt: experimental results and application. Year b.-Carnegie Inst. Wash. 88, 42–47.

Vaselli, O., et al., 1995. Ultramafic xenoliths in plio-Pleistocene alkali basalts from the eastern Transylvanian basin: depleted mantle enriched by vein metasomatism. J. Petrol. 36, 25–53.

Walter, M.J., 1998. Melting of garnet peridotite and the origin of komatiite and depleted lithosphere. J. Petrol. 39, 29–60.

Winterburn, P.A., Harte, B., Gurney, J.J., 1990. Peridotite xenoliths from the Jagersfontein kimberlite pipe: I. Primary and primary metasomatic mineralogy. Geochim. Cosmochim. Acta 54, 329–341.

Woodland, A.B., Kornprobst, J., Wood, B.J., 1992. Oxygen thermobarometry of orogenic lherzolite massifs. J. Petrol. 33, 203–230.

Xue, X., Baadsgaard, H., Irving, A.J., Scarfe, C.M., 1990. Geochemical and isotopic characteristics of lithospheric mantle beneath West Kettle River, British Columbia: evidence from ultramafic xenoliths. J. Geophys. Res. 95, 15879–15891.

Yaxley, G.M., Green, D.H., Kamenetsky, V., 1998. Carbonatite metasomatism in the southeastern Australian lithosphere. J. Petrol. 39, 1917–1930.

Yurimoto, H., Ohtani, E., 1992. Element partitioning between majorite and liquid: a secondary ion mass spectrometric study. Geophys. Res. Lett. 19, 17–20.

Zangana, N.A., Downes, H., Thirlwall, M.F., Marriner, G.F., Bea, F., 1999. Geochemical variation in peridotite xenoliths and their constituent clinopyroxenes from Ray Pic (French Massif Central): implications for the composition of the shallow lithospheric mantle. Chem. Geol. 153, 11–35.

Zhang, R.Y., Liou, J.G., Yang, J.S., Yui, T.-F., 2000. Petrochemical constraints for dual origin of garnet peridotites from the Dabie-Sulu UHP terrane, eastern-central China. J. Metamorph. Geol. 18, 149–166.

Zhou, M.F., Robinson, P.T., Malpas, J., Li, Z., 1996. Podiform chromitites in the Luobusa ophiolite, southern Tibet: implications for melt–rock interaction and chromite segregation in the upper mantle. J. Petrol. 37, 3–21.